JOURNAL OF SPACECRAFT AND ROCKETS
Vol. 46, No. 6, November–December 2009

Qualification of Spacecraft Equipment: Early Prediction of Vibroacoustic Environment

J. Santiago-Prowald*
ESA, 2200 AG Noordwijk, The Netherlands
and
G. Rodrigues†
Université Libre de Bruxelles, B-1050 Brussels, Belgium

DOI: 10.2514/1.42706

This paper proposes a new, flexible, and accurate method for predicting the vibroacoustic environment, which is a driving load case in the development of panel-mounted spacecraft units. This method accounts for the physical parameters that intervene in the dynamically coupled response of units and panels to the impingement of the sound radiated by the rocket engines. Accordingly, it can simplify the costly overdevelopment imposed by testing standards relying on simple mass formulas and significant safety factors. It quickly provides acceleration and force levels for vibration tests, can be applied during any project phase, and allows for the coupling of models with different levels of maturity, while still avoiding the lengthy processing imposed by finite and boundary element tools. It uses impedance/mobility for dynamically condensing panels and units in a compact and modular way. The acoustic load experienced by a panel is characterized by means of physical reasoning based on acoustic diffraction and joint acceptance between the mode shapes and diffuse field. Predicted levels are presented for an actual spacecraft panel coupled with several units, and are compared to detailed vibroacoustic analysis using finite and boundary element methods, test results, and ESA and NASA standards.

Nomenclature

A	=	integrating range of the panel
a	=	circular plate radius, m
$C_F(f)$	=	force dynamic coupling between panel and units
$C_{\ddot{U}1}(f)$	=	acceleration dynamic coupling between panel and units
c	=	speed of sound, m/s
f	=	frequency, Hz
f_{co}	=	cutoff frequency, Hz
$G_r(f)$	=	scaling factor of power spectral density of impinging acoustic field
$\mathbf{G}_{\text{res}}$	=	static residual of panel compliance at interface to units, m/N
g	=	acceleration of gravity, 9.81 m/s^2
$H_n(f)$	=	modal frequency response
$H_{nF}(f)$	=	force modal frequency response
j	=	imaginary unit
$j_{nn}^2(f)$	=	joint-acceptance function
k	=	wave number
L	=	largest side length of a rectangular plate or diameter of a circular plate, m
m	=	mass, kg
p	=	acoustic pressure
p_∞	=	far-field acoustic pressure
$S(f)$	=	structural response power spectral density, g^2/Hz for acceleration and N^2/Hz for force
$S_r(f)$	=	acoustic loading power spectral density, Pa^2/Hz
$S_a(f)$	=	spectrum of sound pressure level specified to mission, Pa^2/Hz
y	=	coordinate in panel
$\ddot{U}_1(f)$	=	acceleration frequency response function
$\bar{Y}_f(f)$	=	flexible part of modal mobility matrix
$\mathbf{Z}_e(f)$	=	impedance matrix of units at the interface points
$\Gamma_{\text{ex}n}(f)$	=	generalized modal force applied to panel
$\rho(y_1, y_2, f)$	=	cross-correlation coefficient of acoustic diffuse field
$\phi_n(y_1)$	=	spatial distribution of mode shape of panel
Φ_{fn}	=	matrix of flexible mode shapes of panel

Subscripts

F	=	force
$\ddot{U}1$	=	acceleration

Superscripts

T	=	transpose
$*$	=	complex conjugate

I. Introduction

INSTRUMENTS and equipment units mounted on spacecraft panels undergo intense vibration levels during liftoff in response to the acoustic field inside the launcher fairing. This acoustic field originates from the rocket engine sound radiation, the turbulent mixing of jets in the atmosphere, and the reflections of sound on ground and launch pads. It is random and broadband in nature and is assumed to be an ergodic and stationary acoustic diffuse field for analysis and testing purposes. The resulting random vibroacoustic environment experienced by the units consists thus of the coupled fluid–structure response of the panel supporting the units to the acoustic excitation. The main physical parameters playing a role in this response are the surface of the panel blocking the acoustic diffuse field, the spatial correlation between the acoustic diffuse field and the panel natural mode shapes, the mass and stiffness of the panel, the mass of the units and their stiffness in the out-of-plane direction, their location, and their dynamic coupling with the panel.

Received 15 December 2008; revision received 4 June 2009; accepted for publication 21 July 2009.

*Project Manager, Structures Section, Engineering and Technology Center, European Space Research and Technology Center; Julian.Santiago.Prowald@esa.int. Member AIAA.

†Research Engineer, Active Structures Laboratory, C.P. 165/42, 50 Avenue F. D. Roosevelt; Goncalo.Rodrigues@ulb.ac.be.

Early knowledge of the vibroacoustic environment is crucial for the equipment development. ESA and NASA standards specify simple formulas that are a function of the mass of the unit alone and which result from the conservative enveloping of the available data. Such a simplification in terms of parameters requires the application of significant safety factors, which leads to overdesigning and overtesting and, thus, increased cost, weight, and schedule.

Several approaches have been proposed that characterize the subsystems in higher detail aiming at more realistic predictions. Various authors have studied the effects of the interaction of the main mode of the panel with the main mode of the unit [1–4]. Ceresetti and Van der Laan additionally considered the influence of the mass per unit area of the panel on the vibroacoustic environment of the units [5].

Fully coupled vibroacoustic analyses relying on the finite element method (FEM) for the structure and the boundary element method (BEM) for the fluid constitute the most accurate tool for vibroacoustic prediction in the low-frequency range, where the modal density is reasonably small. The FEM part consists of a modal analysis of the structure comprising all the subsystems, and the BEM part evaluates how these coupled natural modes of the structure interact with the acoustic field. One simple change on the design parameter will lead to restarting the full process from the beginning. Therefore, this can be critical in an early design phase when the exploration of different configurations is performed, causing delays and excessive effort.

This paper describes an accurate and flexible procedure for predicting the vibroacoustic environment of equipment mounted on spacecraft panels. It is a further development of previous work by the authors [6–8] for computing the coupled dynamic response of spacecraft structures employing the impedance/mobility condensation technique, providing here revised formulations and improved theoretical justifications. The method is based on the separate dynamic characterization of the constituting subsystems. This approach is flexible in the sense that it can be employed in any phase of the project. In early phases of the design, the modal properties of the subsystems can be determined by hand calculations using models of beams and plates or from heritage data from previous projects. As the project progresses, results from FEM modal analyses or subsystems vibration tests can be incorporated. Moreover, the method allows for the coupling of data from different subcontractors, even accommodating different levels of model maturity. At every moment, coupled frequency response functions of the entire system become available, which allow the computation of acceleration and force levels at equipment interface, suitable for vibration test specifications. In this paper, the impedance/mobility condensation technique is complemented with the physical modeling of the acoustic excitation of the mounting panel. This acoustic excitation is itself simplified as the rigid scattering of the acoustic diffuse field by the panel and the quantification of its participation in the excitation of the natural modes by means of the joint-acceptance functions. With this simplification of the acoustic loading of the panel, any new configuration of the instruments and equipment units can be reanalyzed without requiring a new coupled acoustic computation. Despite the fact that this characterization of the acoustic problem does not consider the acoustic radiation, it is still applicable to situations of low-acoustic coupling, which is the case of most spacecraft platform structures. Acoustic radiation is significant though for lightweight structures and appendices, such as solar arrays and antenna reflectors, especially for masses per unit area below 3 $\mathrm{kg/m^2}$ typically. In those cases, the acoustic radiation cannot be neglected and a fully coupled analysis is necessary. The method relies on the following assumptions: negligible acoustic radiation of the structural panel, as explained previously; simply supported panel boundary conditions (quite close to the typical mounts of such panels, especially at high frequencies); and no significant stiffening of the panel by the units (the footprint and the interface stiffness are such that the units behave mainly as a loading mass and a set of oscillators when mounted on the panel). Concerning the transmission of vibrations through panel interfaces, they have been neglected in this study. This is an acceptable procedure for the case of lateral and secondary structure panels of large dimensions, typically 1 m or more, and not connected directly to the launcher interface. However, it is possible to combine both load cases (random vibration through the interface and acoustic excitation) whenever the cross correlation of both inputs is known, or simply by combining the responses in a conservative manner [1].

The outcome of this study is a tool for predicting the vibroacoustic environment of equipment and instrument units from the acoustic specification that can be easily programmed, accounts for the relevant physical parameters of the vibroacoustic problem, and can be employed at any phase of the project. It avoids intensive modeling efforts and heavy computations with FEM/BEM or statistical energy analysis methods and, because it requires only modal data of the subsystems, it is independent from the platforms used by the different subcontractors. It enables the quick computation of sensitivities to changes in the design parameters, in particular to modifications of instrument and equipment units, because the acoustic simulation depends exclusively on the applied sound pressure level and the global geometry and modal properties of the supporting panel.

The proposed method has been validated using as a benchmark the external panel 1B of the structural model of the payload module of the MetOp spacecraft (S/C) and the respective instruments and equipment units. The computed predictions were compared against ESA and NASA random vibration standards, fully coupled FEM/BEM vibroacoustic analyses, and measurement data of system level acoustic tests.

Furthermore, it can be envisaged an application of this method in parallel with the prediction of the response of the panel to base excitation [6]. This will thus provide a complete prediction of the random vibration environment (RVE) for any unit by combining the vibroacoustic and the random accelerations transmitted from the base.

II. Description of the Method

The acoustic environment inside the fairing of a launch vehicle is the major contributing source of the random vibration levels applied to the instruments and equipment units mounted on spacecraft panels. The acoustic radiation can be neglected for secondary spacecraft structures, as will become clear in this paper. By neglecting this aspect of fluid–structure interaction, the entire acoustic environment can be synthesized into an equivalent random and homogeneously distributed pressure load applied to the panel of the spacecraft. The geometrical correlation between this random and homogeneous load and the mode shapes of the spacecraft panel can be quantified by the joint-acceptance functions (JAF) [9]. The random response of the panel can then be written as the superposition of the response of each structural mode scaled by these joint-acceptance functions. Hence, the power spectral density (PSD) of the response of the spacecraft panels to a distributed random loading can be written as

$$S(f) = S_r(f) \sum_{n=1}^{N} H_n(f) H_n^*(f) j_{nn}^2(f) \tag{1}$$

The three terms in Eq. (1) are the PSD of the impinging acoustic field $S_r(f)$, the modal frequency response functions of the coupled panel-equipment structure $H_n(f)$, and the joint-acceptance function $j_{nn}^2(f)$ between the mode shapes of the panel and the acoustic diffuse field.

A. Mechanical Simulation

The authors have shown in previous papers [6–8] the advantages of computing the modal frequency response functions of the structure composed by the spacecraft panel and the equipment units using an impedance/mobility condensation method. In such an approach, each subsystem is characterized in a compact and modular way, and the solution of the coupled dynamic response is obtained by the multiplication of the impedance and mobility matrices. This avoids the eigenvalues extraction to the entire system each time a parameter is modified. Because only basic modal parameters of the units and the panel are required, the method can be applied in any phase of the project. In a preliminary phase, each subsystem can be characterized by simple analytical formulas of modal properties of

beams and plates or by heritage information. In more advanced phases, finite element analysis or test measurement data are usually available. The impedance/mobility condensation technique eases integration of subcontractors' data, enables the quick computation of sensitivities, and allows the prediction of acceleration and force levels for dynamic tests.

The mechanical contribution required to determine the random acceleration response of the panel-equipment structure to the acoustic excitation described by Eq. (1) is the modal frequency response $H_n(f)$. It describes the contribution of the natural mode n of the panel to the acceleration at the I/F points to the equipment under the excitation of the external generalized forces applied to the panel, and the panel being dynamically coupled to the equipment:

$$\ddot{U}_1(f) = \sum_{n=1}^{N} H_n(f)\Gamma_{exn}(f) \tag{2}$$

In [6], the expression of $H_n(f)$ in terms of the modal properties of the panel and equipment units is provided. By neglecting the generalized force from the panel base excitation, which allows restricting the mode shapes and the mobility of the panel to the flexible modes only, and after proper manipulation, the modal frequency response function of the acceleration at the I/F to equipment in response to the loads applied to the panel can be written in the form

$$H_n(f) = j2\pi f C_{\ddot{U}1}(f)\Phi_{fn}^T \bar{Y}_{fn}(f) \tag{3}$$

Where Φ_{fn} are the values of the panel flexible mode shapes at the I/F to the equipment, $\bar{Y}_{fn}(f)$ is the modal mobility matrix of the panel corresponding to the flexible modes, and $C_{\ddot{U}1}(f)$ accounts for the dynamic coupling between the panel and the equipment.

Each component of the vector $H_n(f)$ corresponds to a degree of freedom of the I/F between the panel and the equipment. However, it might be of interest to know the response at other locations of the panel, namely where accelerometers are placed during vibration tests. This only requires the insertion of the values of the mode shapes that correspond to the respective degrees of freedom into Φ_{fn} in Eq. (3).

The matrix of the dynamic coupling $C_{\ddot{U}1}(f)$ is expressed as

$$C_{\ddot{U}1}(f) = I - [\mathbf{\Phi}_f^T \bar{\mathbf{Y}}_f(f)\mathbf{\Phi}_f + j2\pi f \mathbf{G}_{\text{res}}]\{I + \mathbf{Z}_e(f)[\mathbf{\Phi}_f^T \bar{\mathbf{Y}}_f(f)\mathbf{\Phi}_f + j2\pi f \mathbf{G}_{\text{res}}]\}^{-1}\mathbf{Z}_e(f) \tag{4}$$

where $\mathbf{Z}_e(f)$ is the impedance matrix of the equipment and $\mathbf{G}_{\text{res}}$ is the residual of the static flexibility matrix of the I/F points. The physical meaning and the computation of these quantities is thoroughly described in [6]. It can be observed that, in the absence of equipment mounted on the panel, the impedance matrix of the equipment $\mathbf{Z}_e(f)$ becomes zero and the coupling matrix $C_{\ddot{U}1}(f)$ degenerates to the identity matrix. As a result, the modal frequency response function in Eq. (3) will only depend on the mode shapes and the modal mobility of the panel, and Eq. (1) will yield the trivial response of a panel excited by a uniformly distributed random pressure load.

The prediction of the vibration force levels at the equipment I/F could be used for specifying force limiting tests [2,3] and avoiding overdesigning and overtesting the units. The derivation of the modal frequency response function of the forces at the I/F to equipment in response to loads applied to the panel follows the same principles as that of the acceleration [6] and becomes

$$H_{nF}(f) = C_F(f)\Phi_{fn}^T \bar{Y}_{fn}(f) \tag{5}$$

In this case, the matrix describing the dynamic coupling becomes

$$C_F(f) = \{I + \mathbf{Z}_e(f)[\mathbf{\Phi}_f^T \bar{\mathbf{Y}}_f(f)\mathbf{\Phi}_f + j2\pi f \mathbf{G}_{\text{res}}]\}^{-1}\mathbf{Z}_e(f) \tag{6}$$

B. Acoustic Pressure Simulation

The acoustic environment specified for qualification tests of spacecraft is customarily based on the diffuse-field ideal concept, meanwhile, the verification tests are usually performed in large reverberating chambers [10]. The difference between diffuse and reverberant fields is accepted by launch authorities. More difficult to understand is, however, the difference between the actual pressure field within the fairing during launch and a theoretical diffuse field. This difference indeed supports the reverberant chamber test, although the presence of the fairing for reproducing the cavity modes with the spacecraft inside is neither feasible nor representative of the launch conditions, especially when test specifications are produced at early development phases. These difficulties are overcome by the launcher authorities by including large margins in the qualification sound pressure levels. In the end, the definition of pressure fields as a steady, ergodic, wide-band diffuse field appears as the only manageable one for development and also for detailed design tasks.

The purpose of this section is to provide a simplified (although sufficiently accurate and conservative) representation of the actual pressure distribution on the surface of a plate in a diffuse field. Because of the characteristics of the secondary structures and their mass loading, a fully coupled fluid–structure interaction analysis is not necessary most of the times. In particular, the acoustic radiation of the plate can be neglected, while retaining other effects such as air effective mass loading and the rigidly scattered pressure distribution. This approach, for this type of structure, would only affect some of the response peaks by slightly overestimating their amplitudes, while correctly capturing the pressure distribution correlation with structural eigenmode shapes and hence the frequency-dependent force input.

The diffraction of plane waves by rigid plates can be obtained by analytical or numerical integration exploiting spheroidal functions or Rayleigh's formulations, as shown in the classic works of Leitner [11] and Wiener [12]. More recent publications employ Green's formulation [13–15]. The circular and square plates immersed in plane-wave fields are extensively documented for the far field, as well as the surface pressure on the illuminated and shadow sides. In the limiting case of the Kirchhoff approximation (strictly valid for $ka \gg 1$, i.e., short wavelengths compared to the plate size), $p/p_\infty = 1$ in the points of the plane not occupied by the scatterer, up to the edge, $p/p_\infty = 2$ on the illuminated side (perfect reflection) and $p/p_\infty = 0$ on the shadow side (perfect shadow). This crude simplification does not show the diffraction of waves as a function of the wavelength, although it represents already an indication of the pressure blocking of large rigid plates.

The approximation using Rayleigh's integral (distribution of point sources behaving as if located within a rigid infinite baffle; see, e.g., [15]) provides simple closed-form solutions for plane waves of any incidence. In particular, for a plane normal wave on a circular rigid plate, the pressure at the center is [12]

$$\frac{p}{p_\infty} = [(2 - \cos ka)^2 + \sin^2 ka]^{1/2} \tag{7}$$

The solution to Rayleigh's integral for general incidence angle and shape of the scattering plate are provided in Wiener's paper, together with experimental results and the exact solutions based on spheroidal functions. All the expressions obtained, such as Eq. (7), provide interesting information. First, all solutions depend on the similarity parameter $ka = 2\pi fa/c$, which allows for generalization of the solution to any plate size. Second, it can be seen that the Kirchhoff approximation is not good enough for long wavelengths (low frequencies), where, in fact, the excitation of structural eigenmodes can be a dominant factor in the case of spacecraft structures. It can be seen that, for $ka \ll 1$, the plate does not block the incoming wave and is hence transparent to it. Therefore, Kirchhoff's assumption would largely overestimate the response at those low frequencies. The pressure distribution on a radius of the circular plate is maximum at the center, for $ka < 4.5$ approximately [12], and reaches $p/p_\infty = 1$ toward the edge. The shape of the curve changes as ka increases, approaching the Kirchhoff limiting values [11].

The solution in Eq. (7) for the normal plane wave oscillates between $p/p_\infty = 1$ and 3, with the extrema values at $ka = \pi n$. Similar solutions can be obtained for different incidences. In Fig. 1,

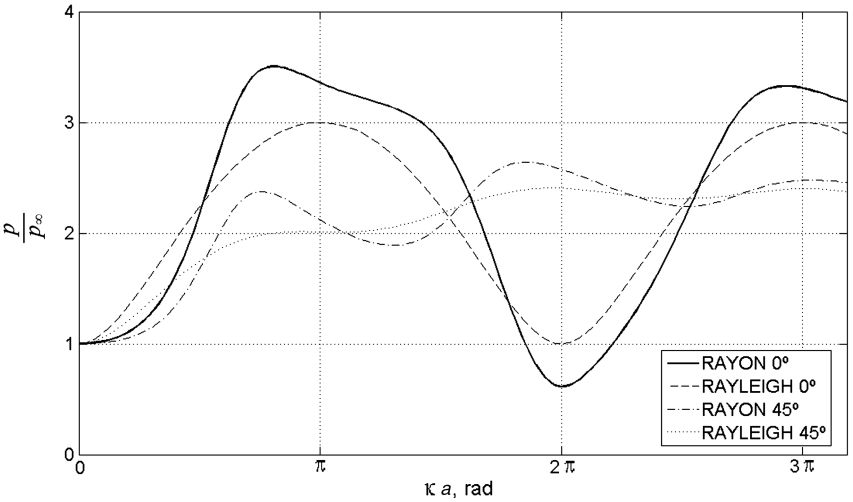

Fig. 1 Pressure at the center of a circular plate of radius a computed with BEM (RAYON) and the Rayleigh integral [10] for a normal and 45 deg incidence.

the Rayleigh integral is compared to the BEM solution obtained with RAYON for the normal incidence and for 45 deg at the center of the circular plate with a unit input. For different incidence angles, the extrema shift in the ka axis and the axial symmetry is lost. This has relevance when computing the pressure distribution curves in a diffuse field, because it can be simulated by superposition of a distribution of plane waves in the 4π sr (steradian) space. In Fig. 2, the pressure curve at the center of the circular plate in a diffuse field (simulated with 26 plane waves uniformly spaced in the 4π sr space, for a 1 Pa^2/Hz white noise random input) is provided as a function of the similarity parameter ka. This result for the scattering of an acoustic diffuse field on a rigid circular plate was already studied by Riobóo et al. [16]. Herein, the same results are compared to the simpler Rayleigh integral as expressed by Wiener in [12].

The actual load input on the plate is the pressure difference across the faces of the panel, that is, the pressure jump. For thin plates in a diffuse field, it can be understood that the phase difference has to be negligible in the low-frequency limit. However, it has been observed by numerical analysis and measurement that the phase difference between both sides and hence the pressure jump, far enough from the edges of the plate, increases with ka [16]. Therefore, the pressure jump at the center of the circular plate is close to a factor 2 of the PSD pressure level on each side, as a worst-case estimation, above a certain frequency. In Fig. 3, the pressure jump across the circular rigid plate at the center is shown as function of ka, for a unit white noise diffuse field, simulated with 62 noncorrelated plane waves uniformly spaced in the 4π sr space. As discussed in the preceding paragraph, the analysis of Riobóo et al. [16] showed that the interaction between the acoustic field and a circular plate occurs mainly at frequencies higher than the so-called cutoff frequency f_{co}, which is a function of the size of the plate. No significant pressure jump arises below f_{co} and hence the excitation of the structure will be very low. Above f_{co}, the pressure blocking is significant and the distribution of the load input evolves from zero pressure jump at the edges to a pressure jump about 4 times the value of the acoustic diffuse field at infinity p_∞.

The same conclusions can be drawn for square and rectangular plates, taking as reference dimension the largest length of the sides. The pressure distribution on the plate surface follows a more complicated pattern than for the circular plate [12]. It is observed, however, as supported by the Kirchhoff and Rayleigh approximations, that the main conclusions are valid for a description of the pressure load as a function of frequency. In particular, the cutoff frequency that establishes the threshold of pressure loading of the panel is defined in terms of the speed of sound and the largest dimension of the panel L:

$$f_{\text{co}} = \frac{c}{2L} \qquad (kL = \pi) \tag{8}$$

For the panel 1B of MetOp, it results in a cutoff frequency of $f_{\text{co}} = 101.2$ Hz. The amplitude of the pressure jump was assumed constant all over the panel (hence applying Kirchhoff's assumption).

For each particular spacecraft, the acoustic environment to be applied in the qualification tests is specified in terms of a sound pressure level (SPL) enveloping all potential launch vehicles to be

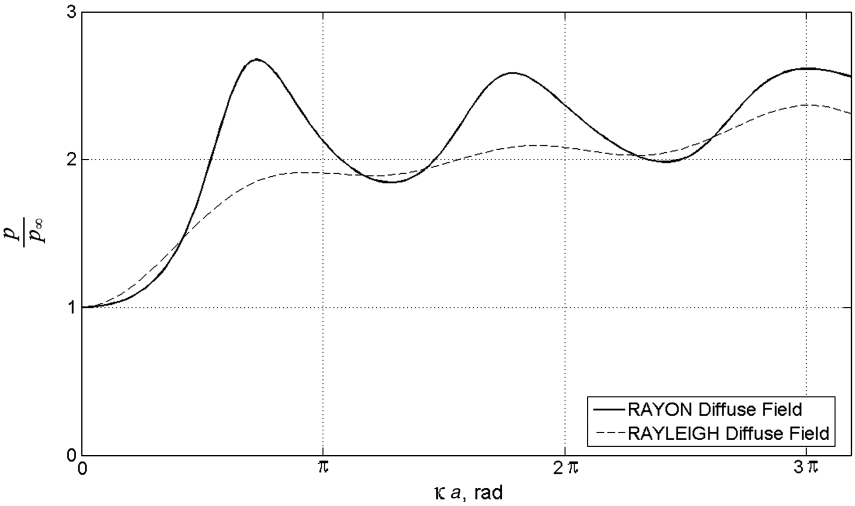

Fig. 2 Pressure PSD at the center of a circular plate of radius a computed with BEM (RAYON) and the Rayleigh integral [10] for the diffuse field.

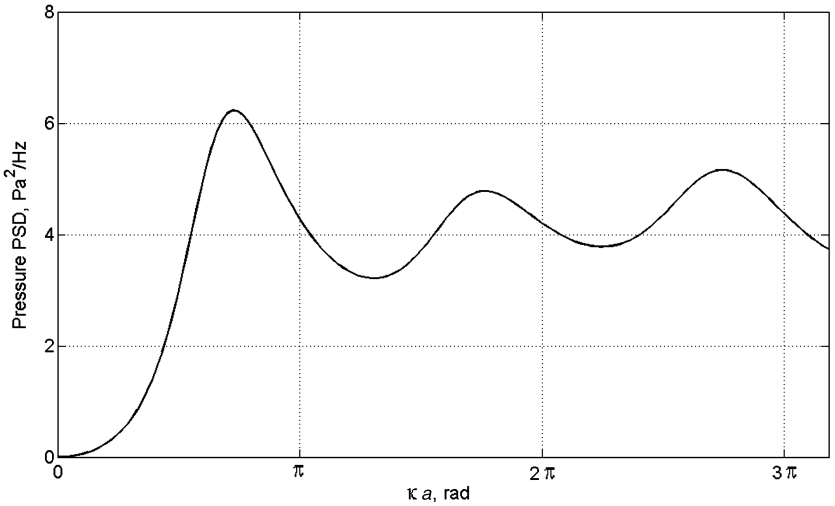

Fig. 3 Pressure jump at the center of a rigid circular plate of radius a in a unitary diffuse field (BEM-RAYON).

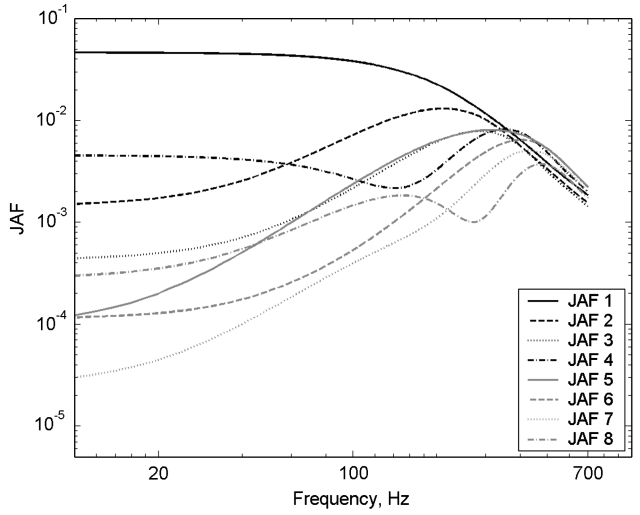

Fig. 4 Joint acceptance between an acoustic diffuse field and the first eight natural modes of MetOp panel 1B.

used. The PSD of the acoustic loading to be inserted in Eq. (1) to compute the acoustic random environment of equipment is thus the product of the SPL specified for the mission by a profile $G_r(f)$, similar to Fig. 3:

$$S_r(f) = G_r(f)S_a(f) \tag{9}$$

C. Joint-Acceptance Function

In a deterministic dynamic excitation, the response of a structural mode depends on the spatial matching between the corresponding mode shape and the applied load. This matching is quantified by the generalized modal forces. The extension of this concept to the random domain is the JAF, which quantifies the spatial correlation between structural mode shapes and the distributed random loading. The JAF is represented by the term $j^2_{nn}(f)$ in Eq. (1) and is defined as the projection of the cross-correlation coefficient of the loading between two points $\rho(y_1, y_2, f)$ on the mode shapes of the structure

$$j^2_{nn}(f) = \int_{A_1}\int_{A_2} \phi_n(y_1)\phi_n(y_2)\rho(y_1, y_2, f)\,\mathrm{d}y_1\,\mathrm{d}y_2 \tag{10}$$

Eckart [17] determined the cross correlation of an acoustic diffuse field between two points of space, and because the diffuse field is homogeneous, the cross-correlation coefficient depends only on the relative distance between the two points:

$$\rho(|y_1 - y_2|, f) = \frac{\sin(k|y_1 - y_2|)}{k|y_1 - y_2|} \tag{11}$$

The JAF between an acoustic diffuse field and the first eight modes of panel 1B of the MetOp S/C were calculated by numerical integration employing Eq. (10) and (11) using the mode shapes of the panel computed by NASTRAN. These are illustrated in Fig. 4. Mode 1 corresponds to the drum mode of the panel and its highest response occurs when the applied pressure is in phase at all the points of the panel. This occurs at zero frequency, when $\rho(|y_1 - y_2|, f)$ is unitary for all the possible combinations of two points on the surface of the panel. All the other mode shapes are characterized by a succession of peaks and valleys and their maximum excitation requires some degree of phase opposition of the applied pressure throughout the surface of the panel, which occurs at nonzero frequencies.

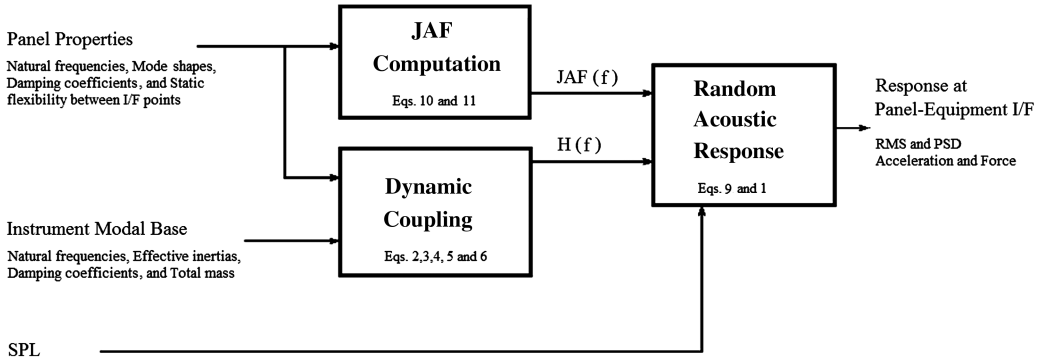

Fig. 5 Data flow for prediction of vibroacoustic environment.

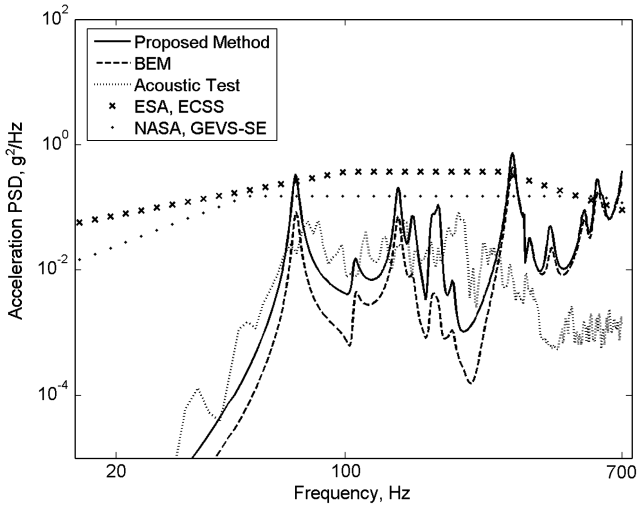

Fig. 6 RVE for MEPED. Comparison between preliminary analytical prediction, BEM, experimental, and ESA/NASA standards.

D. Numerical Implementation

The prediction of the acceleration and forces at the panel-equipment I/F constituting the acoustic environment by means of Eq. (1) requires a discretization of the frequency spectrum, the computation at each frequency point of the modal frequency response functions $H_n(f)$, the PSD of the acoustic loading $S_r(f)$, and the JAF $j^2_{nn}(f)$, as detailed in Secs. II.A–II.C, and the combination of these quantities according to the flowchart of Fig. 5. The evaluation of the JAF for each frequency point from Eqs. (10) and (11) is the heaviest computational step because it requires a double integration on the surface of the panel consisting of four variables. The refinement of the integration grid depends on the desired frequency range. However, several mitigation actions can be envisioned. The cross-correlation coefficient $\rho(|y_1 - y_2|, f)$ can be initially computed and tabulated, and then interpolated during the numerical integration. Also, the adequacy of approximating the two-dimensional JAF by the products of one-dimensional ones or the creation of a database of JAFs for typical panel structures and geometries can be envisioned.

The method presents enough flexibility so that it can be applied at any phase of the design process. SPL are specified at the early stages of the mission development according to the foreseeable launch vehicles to be used. The modal properties of the S/C panel and the equipment can, in an early phase, be obtained by analytical formulas or from heritage from previous projects, and subsequently be updated by results from finite element analysis and structural modal tests as the program evolves.

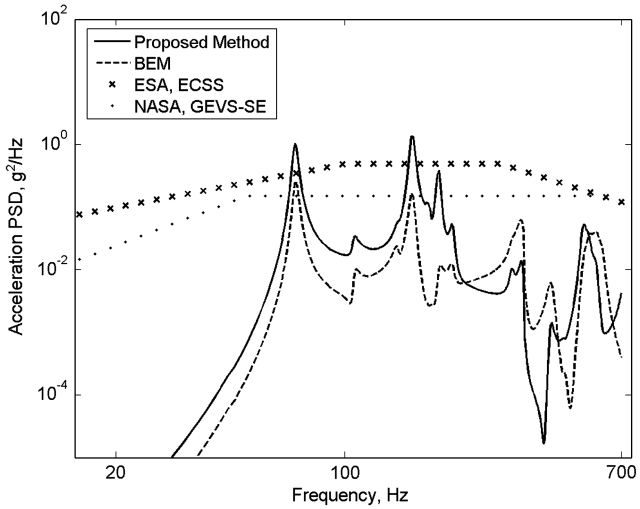

Fig. 7 RVE for EPC-A. Comparison between preliminary analytical prediction, BEM, and ESA/NASA standards.

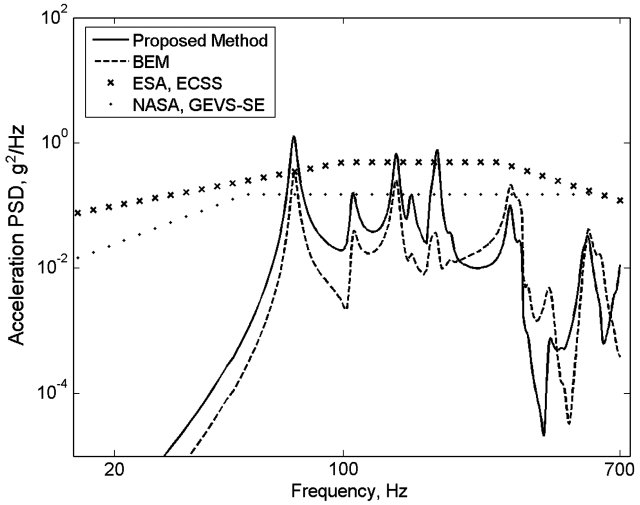

Fig. 8 RVE for EPC-B. Comparison between preliminary analytical prediction, BEM, and ESA/NASA standards.

III. Validation of the Method

This new method has been employed for predicting the out-of-plane vibroacoustic environment of panel 1B of the MetOp spacecraft. Random acceleration levels were determined at the interface points between the panel and instruments and equipment units and compared against the results of a vibroacoustic analysis using the boundary element program RAYON, the levels specified by ESA and NASA standards [18,19], and the experimental measurements obtained during the acoustic qualification test. This comparison is performed in terms of the acceleration PSD and rms.

ESA's MetOp spacecraft structural model was tested in the Large European Acoustic Facility with the objectives of demonstrating that the fully integrated S/C can survive an acoustic test based on the expected launch acoustic environment and establishing the vibro-acoustic response characteristics of the S/C. The structure tested included the platform structure, as well as structural models or mass dummies of equipment units. Several test runs were performed, including acceptance level tests for Soyuz and Ariane and a qualification test at 146 dB, specified over the octave bands up to 2000 Hz. The homogeneity of the acoustic field was controlled with 13 microphones. The spacecraft was instrumented with 252 accelerometers and mounted on a test adapter, screwed to the chamber floor through air bellows for isolation. It has to be noted that the acoustic test involved a full spacecraft, whereas the analyses performed for this paper involve only the panel 1B and its units. The structural panel consists of a honeycomb core sandwich plate.

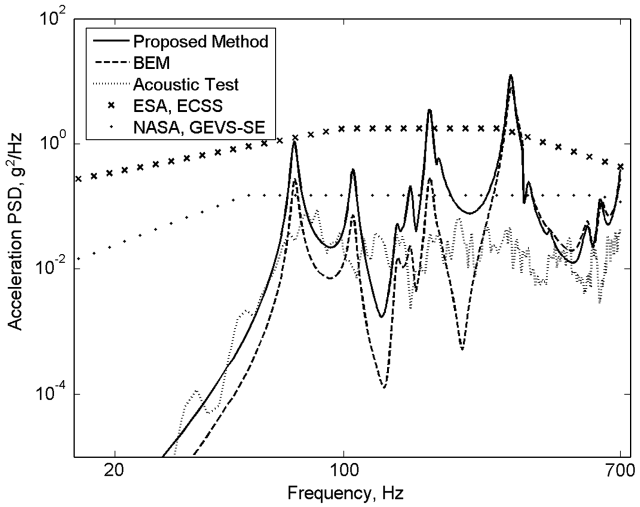

Fig. 9 RVE for DBU. Comparison between preliminary analytical prediction, BEM, experimental, and ESA/NASA standards.

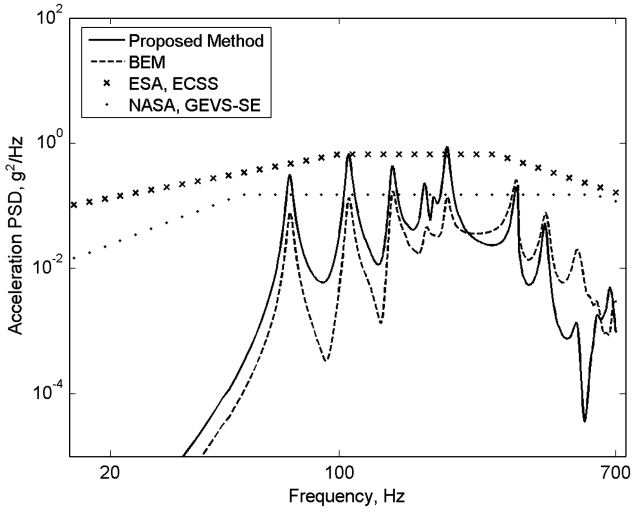

Fig. 10 RVE for SSPA-A. Comparison between preliminary analytical prediction, BEM, and ESA/NASA standards.

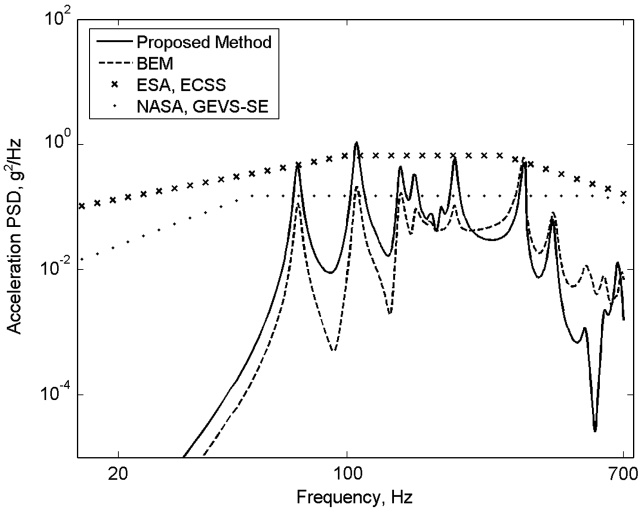

Fig. 11 RVE for SSPA-B. Comparison between preliminary analytical prediction, BEM, and ESA/NASA standards.

The mass of the panel alone is 26.8 kg, including harness [6]. It was considered as simply supported with eight fixed units modeled by springs, masses, and dashpots. Because no antennas or boomlike structures exist on the panel, no rotational motion was considered

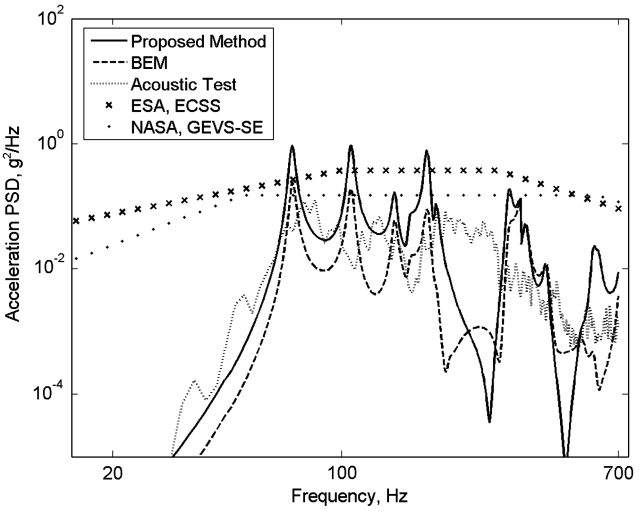

Fig. 12 RVE for MPU. Comparison between preliminary analytical prediction, BEM, experimental, and ESA/NASA standards.

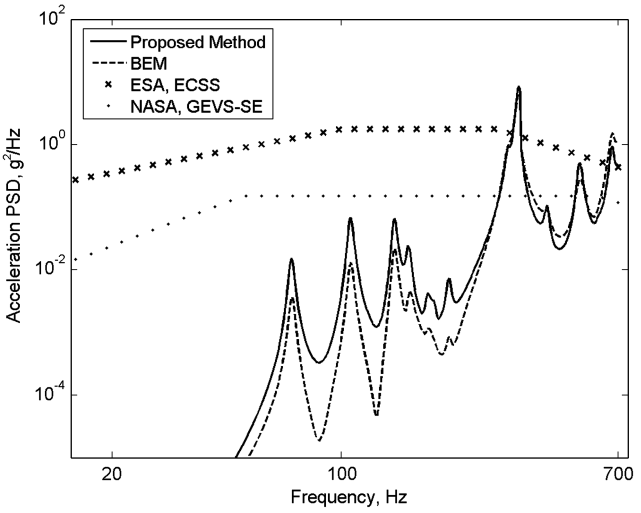

Fig. 13 RVE for HRS. Comparison between preliminary analytical prediction, BEM, and ESA/NASA standards.

and only the out-of-plane component of the panel was retained. According to the impedance/mobility approach, the modal characterizations of each instrument and of the panel are performed independently. The modal base of the panel was extracted up to 4000 Hz by a NASTRAN finite element analysis and considering the added mass of air. The natural frequencies obtained below 1000 Hz are presented in Table 1 and, as can be seen, are lower than those obtained in vacuum in the previous study [6] due to the added mass of air. The modal parameters of the instruments are presented in Table 2 and were established based on similarity to other instruments for which modal information was available and on vibration test results.

The vibroacoustic environment has been predicted using Eq. (1) and following the procedure described in the preceding paragraphs, employing the sound pressure level measured in the acoustic qualification test and presented in Table 3. The vibroacoustic analysis performed with RAYON accounts for the full fluid–structure interaction and consists of two steps. First, the modal base in vacuum of the simply supported panel, dynamically coupled to the instruments, has been extracted with NASTRAN. Finally, the panel has been also discretized with boundary elements for computing the coupled response of the structure to an acoustic diffuse field. This procedure takes into account the pressure blocking and radiation by the panel.

The acceleration levels of the vibroacoustic environment specified by ESA and NASA standards are a function of the mass of the instruments only and are presented in Table 4.

The results in terms of PSD in Figs. 6–13 show that the proposed method provides lower levels for the out-of-plane vibroacoustic environment than those specified by the ESA standards for all the instruments in panel 1B and also those specified by the NASA standards for most of the units. Still, the proposed method remains conservative with respect to the acoustic test results. The correlation of the proposed method with the full vibroacoustic analysis using RAYON is very good and the overpredictions can be explained by the fact that the proposed method does not retain the damping resulting from the acoustic radiation of the panel. It is observed that the acceleration levels measured in the acoustic test are much inferior to those predicted by the proposed method or analyzed with NASTRAN/RAYON. This can be explained by the dynamic coupling between the panel and the primary structure of the spacecraft as well as the uncertainties associated with the modal damping and its variation with the input level.

In Table 5, the rms levels at the interface of the units are compared for the two analytical procedures and the ESA and NASA profiles. It can be observed that the validity of the new method is supported by the fact that it covers the more accurate FEM/BEM prediction, keeping the sensitivity to parameters and a quite good correlation among the analytical methods. Both the ESA-European Cooperation for Space Standardization (ECSS) and NASA-General Environmental

Table 1 Eigenfrequencies of MetOp payload module panel 1B in air

Natural frequency, Hz	Natural frequency, Hz
113.9	687.2
155.7	745.4
218.7	790.5
312.9	812.2
343.7	828.5
398.4	873.5
429.6	890.6
498.7	952.5
522.7	966.9
622.4	993.0
684.3	

Table 2 Modal bases of the instruments mounted on MetOp payload module panel 1B

Instrument	Natural frequency, Hz	Effective mass, kg
MEPED	F1 = 253	0.658
	F2 = 312	1.23
	F3 = 453	2.55
	F4 = 691	0.658
	F5 = 820	1.89
	F6 = 940	1.23
EPC-A	F1 = 464	5.19
EPC-B	F1 = 464	5.19
DBU	F1 = 1249	0.388
SSPA-A	F1 = 1099	3.19
SSPA-B	F1 = 1102	3.19
MPU	F1 = 305	7.98
HRS	F1 = 1250	0.394

Table 3 Spectrum of the sound pressure level of the MetOp qualification acoustic test

Frequency range, Hz	SPL, Pa^2/Hz
[0, 22.3]	421.0
[22.3, 44.6]	383.0
[44.6, 89.1]	376.4
[89.1, 176.8]	431.2
[176.8, 353.6]	74.8
[353.6, 700]	12.1

Verification Specification (GEVS) standards do not retain parameter dependence other than equipment mass. In the case of the NASA standard, there is no variation for the range of masses of the units considered; it specifies always the same input. In general, the new method allows relaxing the levels specified by the standards. There are still overpredictions only for two of the eight units when compared to the NASA standard. These are affecting very low mass units, of less than 0.4 kg, for which the usefulness of the standards is questionable.

Table 4 Standard specifications of random vibration environment (out-of-plane)

ESA-ECSS		GEVS-SE	
Frequency, f	PSD level	Frequency, f	PSD level
[20, 110 Hz]	+3 dB/octave	[20, 50 Hz]	+3 dB/octave
[110, 700 Hz]	0.09 g^2/Hz [a]	[50, 600 Hz]	0.15 g^2/Hz [b]
[700, 2000 Hz]	−5 dB/octave	[600, 2000 Hz]	−5 dB/octave

[a] $\mathrm{PSD} = \begin{cases} 0.12(m+20)/(m+1)\ g^2/\mathrm{Hz}, & m < 50\ \mathrm{kg} \\ 0.09\ g^2/\mathrm{Hz}, & m \geq 50\ \mathrm{kg} \end{cases}$

[b] $\mathrm{PSD} = \begin{cases} 0.15\ g^2/\mathrm{Hz}, & m < 22.7\ \mathrm{kg} \\ 0.15(22.7/m)\ g^2/\mathrm{Hz}, & m \geq 22.7\ \mathrm{kg} \end{cases}$

Table 5 RMS-vibration response, [0, 700 Hz]

RMS, g	New method	FEM/BEM	Experimental	ESA ECSS	NASA GEVS-SE
MEPED	6.60	5.52	2.57	12.8	9.92
EPC-A	5.12	3.03	N/A	14.7	9.92
EPC-B	5.14	3.96	N/A	14.7	9.92
DBU	17.25	14.37	3.55	28.0	9.92
SSPA-A	5.50	4.36	N/A	17.2	9.92
SSPA-B	6.10	5.36	N/A	17.2	9.92
MPU	5.31	2.86	3.22	12.9	9.92
HRS	13.7	14.4	N/A	28.0	9.92

IV. Conclusions

A simple and accurate tool for predicting the random vibration environment from acoustic specifications has been developed for panel-mounted instruments and equipment units. It is based on impedance/mobility condensation techniques that allow the dynamic condensation of all the subsystems separately and a simulation of the acoustic loading consisting of the rigid scattering and joint acceptance of an acoustic diffuse field. The random vibration environment is predicted in terms of acceleration levels at the interface for conventional vibration tests of the units and interface forces for force limited vibration tests. This method accounts for the physical aspects involved in the vibroacoustic response of a spacecraft panel and the mounted instruments and equipment units. These are the applied sound pressure level, the surface of the panel blocking the acoustic diffuse field, the spatial correlation between the acoustic diffuse field and the panel natural mode shapes, the mass and stiffness of the panel, the mass of the units and their stiffness in the out-of-plane direction, the position of the units on the panel, and the dynamic coupling between all the units and the panel.

A simplified prescription of the pressure jump is provided in terms of the characteristic size of the plate, thanks to the similarity parameter kL, which involves the wave number and the size of the panel. The cutoff frequency has been identified for circular and rectangular plates. The pressure load profile and distribution obey the fundamental rigid scattering laws. As shown by simplified integration, this prescription follows rather closely to the more complex numerical integration using boundary element methods and the experimental results. The hypothesis of negligible acoustic radiation has been verified in terms of a conservative peak response prediction.

This method is applicable in any phase of the project. In the preliminary design, the modal properties of the subsystems can be estimated from heritage information from previous projects or by hand calculations of the modal properties of plates and beams. As the project progresses, results from modal finite element method analysis and vibration test results can be incorporated as they become available. Moreover, it incorporates the modal characterization of the different subsystems being developed by different subcontractors, with different levels of maturity and obtained using different platforms. It enables the quick assessment of the impact of design modifications requiring a much lower effort in modeling and computational resources than those required by fully coupled vibroacoustic analyses based on FEM/BEM, as it involves only the multiplication and the inversion of small matrices.

A very good correlation was observed when comparing the proposed method with the results of a FEM/BEM vibroacoustic analysis in the prediction of the vibroacoustic environment for panel 1B of the MetOp spacecraft. It provided overpredictions due to the fact that the damping caused by the panel acoustic radiation is not modeled in the proposed approach.

The proposed method presents still a high level of conservatism with respect to the results of the system level acoustic test, but constitutes a very significant improvement in relation to the ESA and NASA specifications which depend only on the mass of the units.

The mismatch observed between the system level acoustic test and the predictions using the proposed method and the coupled vibro-acoustic analysis using FEM/BEM occur specially at the high frequencies and most likely stem from differences on the structure being modeled and the structure being tested. On the other hand, the hypothesis of dynamic independence of the panel to the primary structure of the spacecraft should probably be further investigated, on what concerns the boundary conditions of the panel and their impact on the modal base, and the dynamic coupling between the panel and the primary structure. The condensation of the primary structure of the spacecraft could also be envisaged in a future study.

Acknowledgments

The authors wish to thank the Portuguese Foundation of Science and Technology for the traineeship program in the ESA and Technology Center (grant SFRH/BEST/7289/2002), and Graham Coe, Hans Van de Graaf, and Ivan Ngan for the kind support.

References

[1] Ceresetti, A., "Limit Load Factors Curve (LLF) for Preliminary Mechanical Design of Components for Space Missions: An Attempt of Mathematical Justification.," *European Conference on Spacecraft Structures, Materials and Mechanical Testing*, ESA, SP-428, 1998, pp. 179–186.

[2] Chang, K. Y., "Force Limit Specifications vs. Design Limit Loads in Vibration Testing," *Proceedings of the European Conference on Spacecraft Structures, Materials and Mechanical Testing*, ESA, SP-468, 2000, pp. 295–300.

[3] Scharton, T. D., "Force Limited Vibration Testing Monograph" NASA RP-1403, May 1997.

[4] Soucy, Y., and Côté, A., "Reduction of Over-Testing During Vibration Tests of Space Hardware," *Canadian Aeronautics and Space Journal*, Vol. 48, No. 1, 2002, pp. 77–86.

[5] Ceresetti, A., and Van der Laan, T., "(L.L.F.) Curves and PSD Derivation Method for Equipment Mounted on Satellite Panels," *Proceedings of the European Conference on Spacecraft Structures, Materials and Mechanical Testing* [CD-ROM], Centre National d'Etudes Spatiales, Toulouse, France, 2002.

[6] Rodrigues, G., and Santiago-Prowald, J., "Qualification of Spacecraft Equipment: Random-Vibration Response Based on Impedance/Mobility Techniques," *Journal of Spacecraft and Rockets*, Vol. 45, No. 1, pp. 104–115. doi:10.2514/1.29734, Jan.–Feb. 2008.

[7] Rodrigues, G., and Santiago-Prowald, J., "Random Vibration Environment Derived from Acoustic Specifications," AIAA Paper 2004-2834, 2004.

[8] Santiago-Prowald, J., and Rodrigues, G., "An Impedance/Mobility Condensation Method For Preliminary Vibro-Acoustic Analysis," *Proceedings of the European Conference on Spacecraft Structures, Materials and Mechanical Testing*, ESA, SP-581, 2005.

[9] Bendat, J. S., and Piersol, A. G., *Engineering Applications of Correlation and Spectral Analysis*, Wiley, New York, 1993.

[10] "Ariane 5 User's Manual," No. 3, Rev. 0, Arianespace, Washington, D.C., 2000.

[11] Leitner, A., "Diffraction of Sound by a Circular Disk," *Journal of the Acoustical Society of America*, Vol. 21, No. 4, 1949, pp. 331–334. doi:10.1121/1.1906517

[12] Wiener, F., "The Diffraction of Sound by Rigid Disks and Rigid Square Plates," *Journal of the Acoustical Society of America*, Vol. 21, No. 4, 1949, pp. 334–347. doi:10.1121/1.1906518

[13] Huang, Ch.-J. and Chwang, A., "Diffraction of Acoustic Waves by Rigid Plane Baffles," *Journal of the Acoustical Society of America*, Vol. 95, No. 2, 1994, pp. 668–680. doi:10.1121/1.408427

[14] Junger, M. C., and Feit, D., *Sound, Structures and Their Interaction*, MIT Press, Cambridge, MA, 1972.

[15] Fahy, F., *Sound and Structural Vibration, Radiation, Transmission and Response*, Academic Press, London, 1985.

[16] Riobóo, J. L., Santiago-Prowald, J., and Garcia-Prieto, R., "Qualitative Vibroacoustic Response Prediction of Antenna-Like Structures During Launch into Orbit," *Proceedings of the European Conference on Spacecraft Structures, Materials and Mechanical Testing*, C. Stavrinidis, A. Rolfo, and E. Breitbach (eds.), ESA, ESASP-468, 2001.

[17] Eckart, C., "The Theory of Noise in Continuous Media," *Journal of the Acoustical Society of America*, Vol. 25, No. 2, 1953, pp. 195–199. doi:10.1121/1.1907018

[18] "Space Engineering: Testing," European Cooperation for Space Standardization, ECSS-E-10-03A, 2002, www.ecss.nl.

[19] "General Environmental Verification Specification for STS & ELV Payloads, Subsystems, and Components," *General Environmental Verification Specification-SE*, NASA Goddard Space Flight Center, Greenbelt, MD, 1996.

G. Agnes
Associate Editor